Structure and Properties of Melt-Extruded LaRC-IA (3,4′-ODA 4,4′-ODPA) Polyimide Fibers

K. D. DORSEY,[1] P. DESAI,[1] A. S. ABHIRAMAN,[1] J. A. HINKLEY,[2] T. L. ST. CLAIR[2]

[1] School of Chemical Engineering, Polymer Education & Research Center, Georgia Institute of Technology, Atlanta, Georgia 30332-0100, USA

[2] Mail Stop 226, NASA Langley Research Center, Hampton, Virginia 23681-2199, USA

Received 18 August 1998; accepted 23 September 1998

ABSTRACT: LaRC-IA polyimide fibers were extruded from the melt and drawn. The fibers were characterized by sonic pulse propagation, polarized optical microscopy, calorimetric analysis, X-ray diffraction, and tensile testing. When the amorphous, essentially isotropic, as-extruded filaments were heated slowly in a calorimeter, no "cold" crystallization could be detected. However, when these filaments were drawn at temperatures above the T_g of the polymer, they crystallized rapidly to produce oriented semicrystalline structures. The consequent increases in modulus and strength were significant, with the properties reaching the levels of commercial fibers of intermediate tenacity. © 1999 John Wiley & Sons, Inc. J Appl Polym Sci 73: 1215–1222, 1999

Key words: LaRC-IA polyimide fibers; melt extrusion; crystallization

INTRODUCTION

Aromatic polyimides are known for their chemical resistance, excellent mechanical and electrical properties, and outstanding thermal stability. Polyimide fibers are expected to have attractive heat resistance and low flammability.[1]

Polyimides are usually prepared via the reaction of a dianhydride with an aromatic diamine in a polar aprotic solvent. In the so-called two-step process, the soluble polyamic acid is fabricated into a product, such as fiber, film, or coating, and then it is converted in a second process to the imide—usually by heating in the vicinity of 300°C. If instead the polyamic acid is thermally or chemically imidized in solution, the polyimide may stay in solution or, more often, precipitate as a powder.

Although most polyimide research to date has concentrated on films, coatings and laminates, a few attempts at fiber production have been reported. Irwin dry-spun various polypyromellitimide precursor fibers from polyamic acid solutions. The polyamic acid fibers were thermally converted to the polyimide under tension and further drawn at 550°C.[2,3] Kaneda et al.[4] spun polyamic acids from 3,3′,4,4′-biphenyltetracarboxylic dianhydride in *p*-chlorophenol into a coagulating bath of ethanol. Solution spinning and coagulation of fluorinated polyamic acid solutions and polyimide resins were previously accomplished at NASA Langley Research Center.[5] Sroog[6] summarizes reports of various polyimide fibers fabricated from polyamic acid solutions and subsequently converted or drawn at temperatures ranging from 340 to 550°C. Eashoo and co-workers[7] have described dry-jet wet spinning of soluble polyimides from hot *m*-cresol.

Melt spinning can be much simpler, since it eliminates the need for coagulation, solvent removal, and separate imidization steps. The

Correspondence to: A. S. Abhiraman.

Journal of Applied Polymer Science, Vol. 73, 1215–1222 (1999)
 CCC 0021-8995/99/071215-08

Table I Properties of As-Extruded Fibers

Sample	Take-Up (m/min)	Denier[a]	Tenacity (g/denier)	Elongation (%)	Avg. Filament Diameter (μm)
A	6.4	329	1.38	224	190
B	6.4	552	1.17	207	250
C	6.4	162	1.32	210	130
D	8.8	131	1.32	172	110

[a] Denier is the linear density of fibers expressed as g fibers/9000 m length.

present research deals with drawing-induced orientation and crystallization of melt-extruded LaRC-IA fibers and the consequent evolution of properties. LaRC™-IA (**I**) is the reaction product of 3,4′-oxydianiline (3,4′-ODA) and 4,4′-oxydiphthalic anhydride (ODPA).[8,3] It can be prepared in a variety of suitable solvents or via direct melt polymerization of the monomers. Preparation and properties of the amorphous melt-spun fibers have been described by Fay et al.[9]

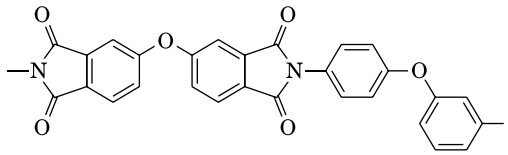

I

EXPERIMENTAL

Material

The LaRC-IA powder was produced by Imitec, Inc. (Lot No. 041-093). The powder was dried for 24 h in a vacuum oven at 100°C prior to extrusion. A laboratory-scale (100 g) vacuum extruder[10] allowed removal of entrapped air and volatiles and extrusion of the polymer through an eight hole die with 0.0135-inch diameter holes at 350°C. Several batches of fibers were produced, with the extruder output and the fiber take-up speed varied to give filament linear densities in the range of 130–550 g/9000m (i.e., 130–550 denier), corresponding to filament diameters in the range of 100–250 μm. Characteristics of the as-extruded fiber are given in Table I. It should be noted here that small-scale extrusions typically result in large variations in filament sizes and so the properties of the resulting filaments are likely to be significantly lower than those that can be obtained from optimized large-scale fiber extrusion.

Drawing Experiments

Two kinds of drawing experiments were carried out: (a) the thermal deformation analysis experiment (TDA), i.e., a nonisothermal simulation of drawing at a constant force, and (b) continuous drawing.

In TDA, two Kevlar yarns were attached to a test fiber loop. With the test fiber loop enclosed in a tube furnace initially at room temperature, one of the yarns was attached to a fixed support, while the other end was passed over a pulley with a specified weight hanging from its end. A video camera recorded the position of the weight relative to a fixed scale as the temperature was increased from room temperature at 10°C/min. The deformation of the fiber loop under the influence of the constant applied force was obtained, as a function of temperature, from the recorded changes in the position of the weight. Contributions from thermal expansion and deformation of the Kevlar yarn in this experiment were negligible.

The continuous drawing apparatus consisted of feed and draw godet rolls, with a tubular oven in the path of the yarn between them. In all the drawing experiments, the speed of the feed godet was held at 0.48 m/min; the maximum draw ratio was determined by slowly increasing the speed of the draw godets until broken filaments were seen. The furnace in the drawing zone was maintained at 250°C.

Mechanical Testing

Sonic modulus was computed from the sonic velocity, measured with the Dynamic Modulus Tester PPM-5 (H. M. Morgan Co.) A small weight was suspended from the yarn to ensure that the filaments made good contact with both transducers. Sonic modulus E, expressed in g/denier, is related to sonic velocity c (km/s) by $E = 11.3\ c^2$.

Stress–strain curves were obtained using the Instron tensile tester model 1121. The number of filaments in the samples ranged from 3 to 8. A gauge length of 6.25 mm and an elongation rate of 10%/min were employed.

Orientation- and Crystallization-Related Measurements

Differential Scanning Calorimetry (DSC)

The calorimetric measurements were carried out using a Seiko SSC/5200 DSC, calibrated with indium. Small quantities of knotted fiber (less than 10 mg) were sealed in aluminum pans. An empty sealed pan served as reference.

Refractive Index and Birefringence

Birefringence was measured with an Aus Jena Interphako transmitted light interference microscope, using light of wavelength 550 nm. Immersion liquids of refractive index in the range 1.648–1.800 were used.

From $n_{\parallel}$ and $n_{\perp}$, the refractive indices with polarization parallel and perpendicular to the fiber axis, the isotropic refractive index n_{iso}, birefringence Δn, and the relative optical density ρ_R were obtained as follows:

$$n_{iso} = 1/3\ (n_{\parallel} + 2\ n_{\perp})$$

$$\Delta n = (n_{\parallel} - n_{\perp})$$

$$\rho_R = [(n_{\mathrm{iso}})^2 - 1]/[(n_{\mathrm{iso}})^2 + 2]$$

Wide Angle X-ray Diffraction (WAXD)

Fiber samples were wound on manila paper frames. Wide angle θ–2θ scans (meridional and equatorial) and azimuthal scans at constant scattering angle were obtained in the transmission mode using a Rigaku-Rotaflex diffractometer with Ni-filtered CuKα radiation. Flat plate photographs were taken with a Molecular Dynamics Imaging Plate in a Statton-type flat plate camera with Ni-filtered CuKα radiation and 0.015 inch diameter pinhole collimation.

RESULTS AND DISCUSSION

Thermal Deformation Analysis

Indirect evidence of orientation-induced crystallization was initially observed in the nonisothermal TDA experiments (Fig. 1). At the lowest load employed, fiber elongation began in this experiment when the temperature was increased to ~200°C, with rapid deformation occurring around 250°C, followed by arresting of this deformation, apparently due to the onset of crystallization. With further increase in temperature, the fiber broke due to melting. As expected, the temperatures corresponding to each of these characteristic phenomena decreased with increase in the tension applied to the filaments. The changes observed are consistent with those observed previously with semiflexible poly(ethylene terephthalate) fibers.[11]

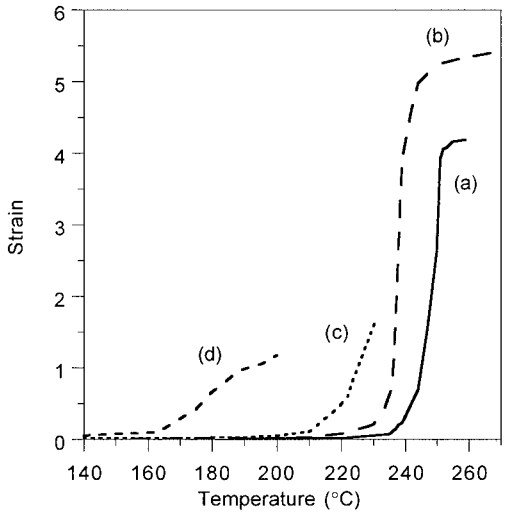

Figure 1 Nonisothermal deformation analysis of as-spun LaRC-IA fibers. Loads applied: (a) 10, (b) 50, (c) 100, and (d) 200 g.

Continuous Drawing

Each batch of fiber was drawn to several draw ratios. The maximum draw ratio used in each case was just below the level at which broken filaments were first detected. Due to the propensity for premature failure of the smaller filaments of a bundle, samples with large variations in fiber diameter had smaller maximum draw ratios. Thus, the properties reported in the following can be significantly improved through processing under more optimum conditions. The highest draw ratio attained was 5.8, with a birefringence higher than could be measured with the available refractive index solutions.

Typical stress–strain curves of as-spun and drawn fibers are shown in Figure 2. The as-spun fibers exhibit a clear yield point, with a large

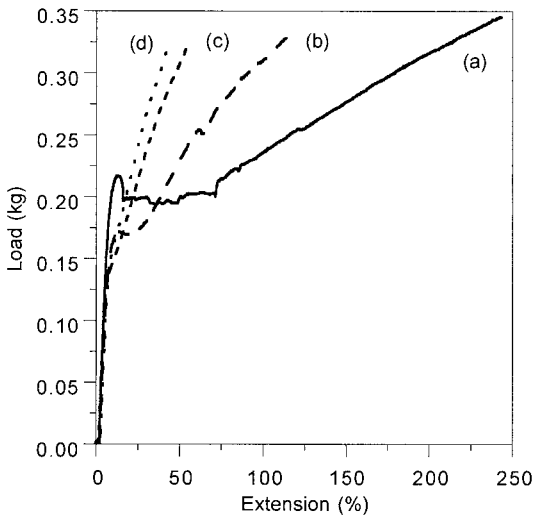

Figure 2 Representative load-elongation curves of LaRC-IA fibers (a) as-spun fibers, (b) draw ratio = 1.11, (c) draw ratio = 2.03, (d) draw ratio = 4.06, and (e) draw ratio = 4.93.

degree of cold drawing and the usual strain hardening. The drawn, crystallized fibers do not show a yield point (relative maximum in load). Elongation at break decreased significantly with increasing draw ratio.

As expected, tenacity increased and the elongation to failure decreased monotonically with increasing extent of drawing (Fig. 3). Variations in individual filament diameters contributed to a large variation in the measured tenacities. However, in spite of the lack of process optimization, the tenacity achieved with the LaRC-IA fibers here is comparable to those of intermediate-tenacity fibers of polypropylene, polyethylene terephthalate, Nomex, and nylon- 6,6 (Table II).

Table II Comparison of the Tenacity of Drawn LaRC-IA Fibers with Typical Textile Fibers

	Average Tenacity (g/denier)
Polypropylene	7.0 (±2.0)
Polyester	5.0 (±1.0)
Nomex	5.0 (±0.6)
Nylon	6.5 (±2.0)
LaRC-IA	5.0 (±0.5)

Drawing-Induced Orientation and Crystallization

Evolution of order during high temperature drawing is a consequence of three competing fundamental processes—stress-induced orientation, relaxation of orientation in noncrystalline segments, and crystallization.[11] Increased orientation and crystallization with drawing led to increase in sonic modulus (Fig. 4), especially beyond a draw ratio of 2.5. Initiation of crystallization marks a lower bound for the level of deformation at which relaxation of orientation is arrested. The birefringence-draw ratio plot (Fig. 5) is typical of the response expected from

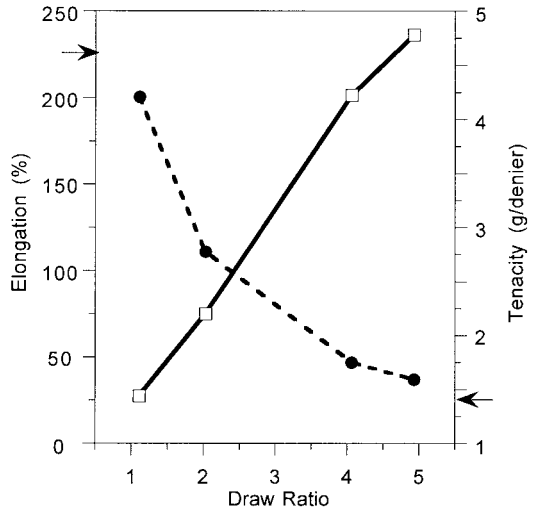

Figure 3 Tenacity (g/denier, open squares) and percent elongation to break (filled circles) as function of draw ratio for sample A. Values for the as-spun fiber are shown by arrows for comparison.

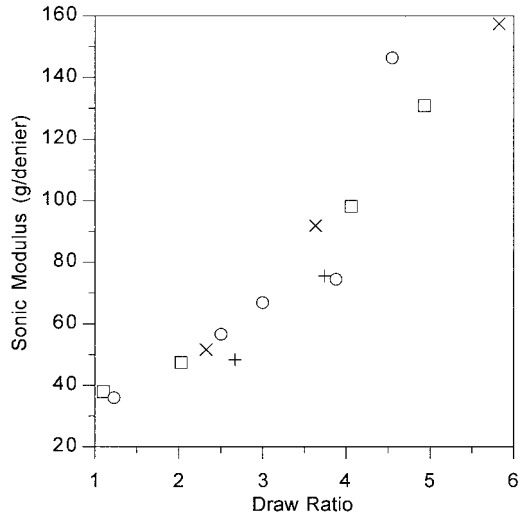

Figure 4 Increase in sonic modulus with draw ratio of drawn LaRC-IA fibers. Symbols correspond to different batches of as-spun fibers.

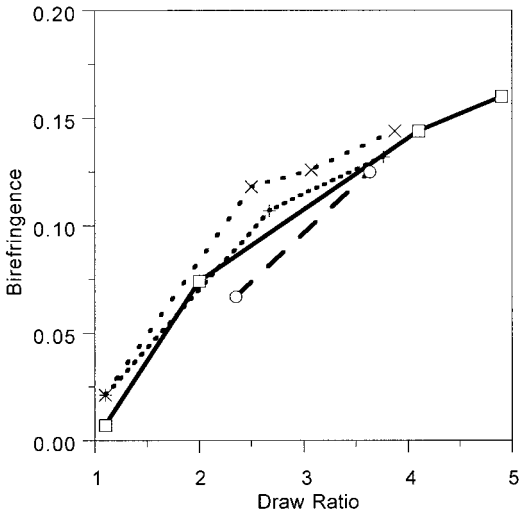

Figure 5 Birefringence of drawn LaRC-IA fibers. Symbols correspond to different batches of as-spun fibers.

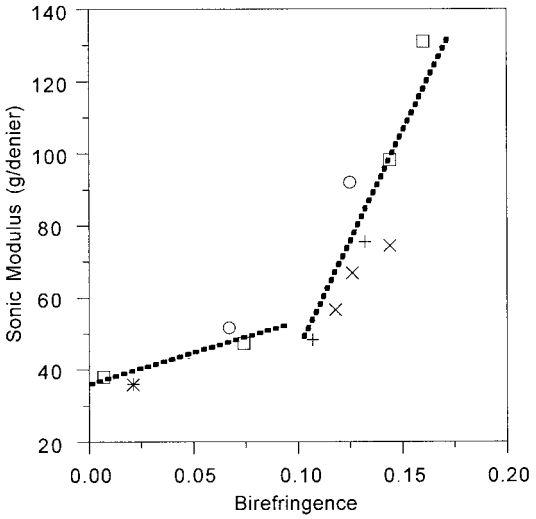

Figure 7 Relationship between sonic moduli and fiber birefringence. Symbols correspond to different batches of as-spun fibers.

an initially amorphous polymer that crystallizes during drawing. Both drawing-induced orientation and orientation-enhancing anisotropic crystallization occur. Beyond a critical draw ratio (~2.5 in this case), the additional orientation with drawing is essentially due only to an increase in noncrystalline orientation. Relative optical density was found to increase with increasing draw ratio, consistent with the formation of crystalline regions by drawing (Fig. 6). It should be noted here that the decrease in $n_\perp$ with increasing draw ratio would imply a decrease in the corresponding component of the dielectric constant, an aspect which could be advantageous in some applications of these polyimides as oriented films and fibers.

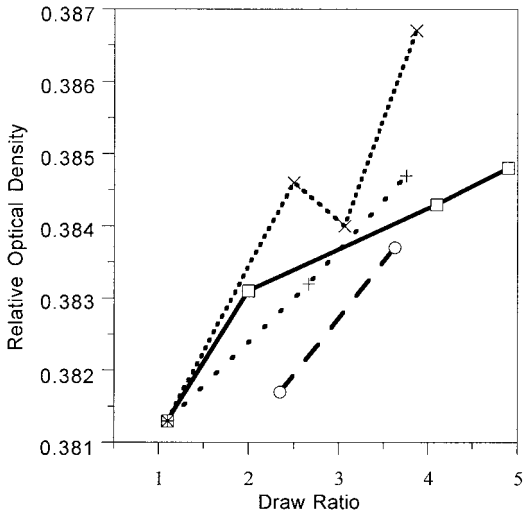

Figure 6 Relative optical density of drawn LaRC-IA fibers. Symbols correspond to different batches of as-spun fibers.

A plot of sonic modulus vs birefringence (Fig. 7) also shows the pronounced influence of the combination of oriented crystallization and relaxation/increase in noncrystalline orientation during drawing of the initially amorphous fibers. In uniaxially oriented polymers, birefringence is strongly influenced by the oriented crystalline fraction whereas the sonic modulus is dictated to a greater extent by the orientation of the noncrystalline fraction. Drawing an initially amorphous fiber to low draw ratios can result in at most a moderate increase in noncrystalline orientation due to the combination of simultaneous relaxation of orientation and preferential crystallization of the more oriented segments. However, the constraints from the crystals which serve to prevent orientational relaxation at higher draw ratios lead to the development of a higher orientation in the noncrystalline phase. Thus we observe the break in the sonic modulus–birefringence relationship depicted in Figure 7.

Typical DSC thermograms of as-spun and drawn fibers are shown in Figure 8. The thermogram of the undrawn fiber indicates only the T_g at ~ 220°C and no melt transition. The absence of any "cold crystallization" exotherm in this case shows that the intrinsic rate of quiescent crystallization of this polymer is extremely low. The

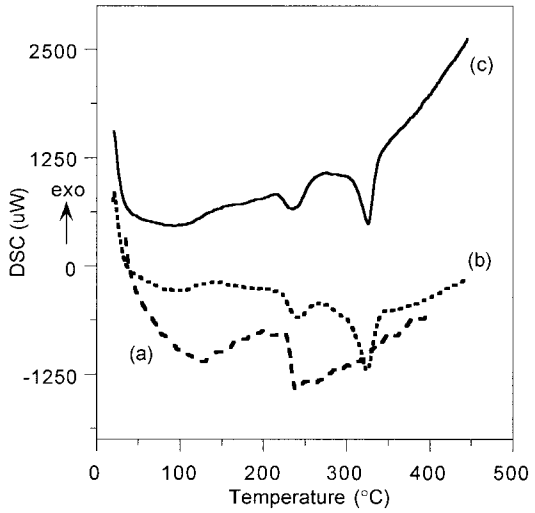

Figure 8 DSC thermograms of as-spun and drawn LaRC-IA fibers (a) as-spun, (b) draw ratio = 3.9, and (c) draw ratio = 5.

drawn fibers show a smaller step change in heat capacity at T_g and a pronounced melting endotherm with a peak T_m at ~ 320°C, showing that a significant level of orientation-assisted crystallization had occurred during drawing.

The meridional WAXD scan of a drawn sample is shown in Figure 9. It is clear that the drawn fiber is well crystallized, with several diffraction peaks. The equatorial WAXD scan (Fig. 10) is broad with high peak intensity. Comparison of these two scans indicates that the order in the drawn fibers is essentially along the chain direction. The equatorial reflection is indicative of a "nematic liquid-crystal like" order. Azimuthal scans (Fig. 11) were made of the meridional reflection at $2\theta = 25.2°$, which had no equatorial interference. The equatorial, meridional, and azimuthal scattering profiles as well as the flat plate wide angle X-ray scattering photographs (Fig. 12) show that these fibers exhibit the following characteristics:

- All the undrawn fibers are essentially isotropic.

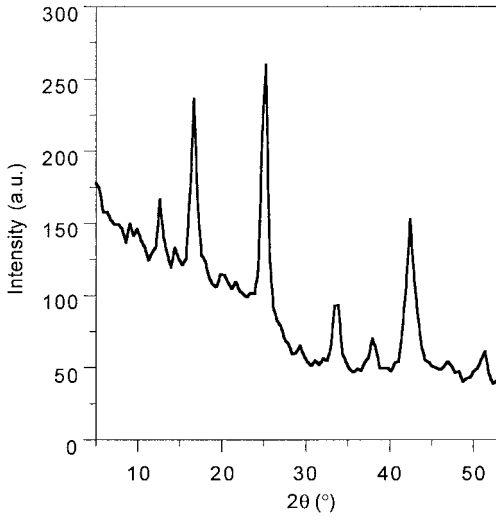

Figure 9 Meridional WAXD scan of LaRC-IA fiber Sample C, drawn to a draw ratio of 4.6.

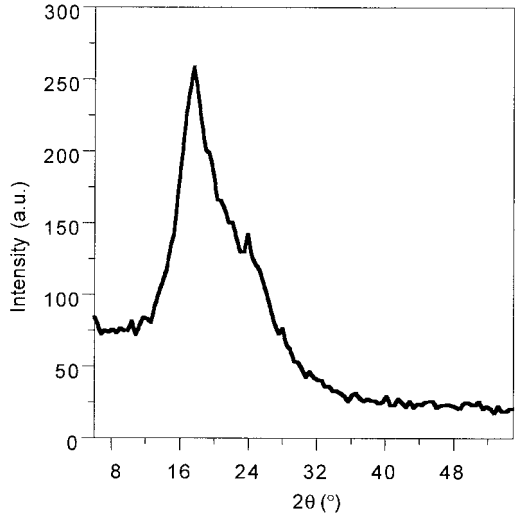

Figure 10 Equatorial WAXD scan of LaRC-IA fiber Sample C, drawn to a draw ratio of 4.6.

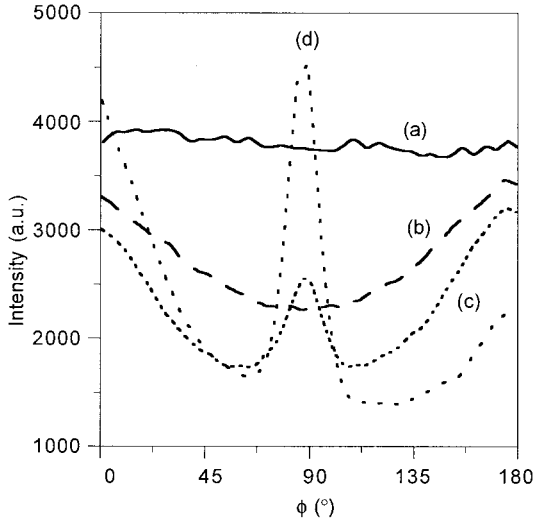

Figure 11 Azimuthal WAXD scans at 25.2° 2θ of LaRC-IA Sample A fibers drawn to various ratios (a) through (d) refer, respectively, to draw ratio of 1, 2, 4, and 4.9.

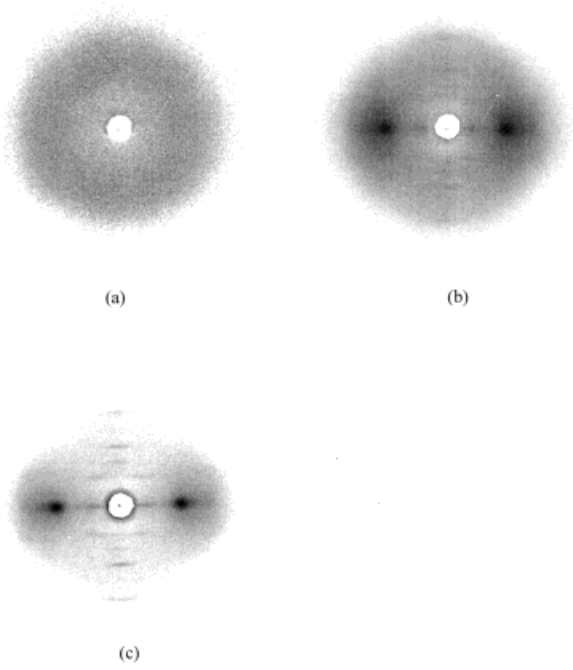

Figure 12 Wide angle X-ray flat plate photographs of as-spun and drawn LaRC-IA fibers (a) as-spun fibers, (b) draw ratio = 3.9, and (c) draw ratio = 5. Fiber axis is vertical.

- At low draw ratios, a preferred orientation develops along the fiber direction, with little crystallization.
- At higher draw ratios, the fibers develop highly oriented crystals that produce the sharp meridional peaks, a higher peak intensity in the broad equatorial scattering, and a significant narrowing of the azimuthal intensity profile.

It is well known that annealing of oriented polymers often promotes further crystal growth and oriented crystallization, while simultaneously decreasing amorphous orientation. Therefore, a sample of highly drawn fiber was annealed at 275°C for 7 min under constraint. Dynamic mechanical analysis showed that, compared to an unannealed sample, the annealed fiber exhibited a significantly lower tan δ (a maximum of ~ 0.3 vs ~ 0.5; Fig. 13a) and much lower shrinkage until the onset of melting, 3–4% compared to 18% shrinkage for the unannealed sample (Fig. 13b).[12] Thus the anisotropy-assisted crystallization, in combination with annealing at a temperature substantially higher than T_g, allows the formation of a structure that provides significant level of dimensional stability at high temperatures.

CONCLUSIONS

Under quiescent conditions, the thermoplastic LaRC-IA polyimide, (3,4′-ODA 4,4′-ODPA), had been known to crystallize only under two conditions, namely, during polymerization or when cast from a solvent. The research reported here was undertaken to determine the feasibility of producing an oriented, crystalline fiber of this polymer through a melt-based process. Towards this end, LaRC-IA was successfully melt spun and drawn, albeit under conditions that are likely to be far from optimum. The following was found:

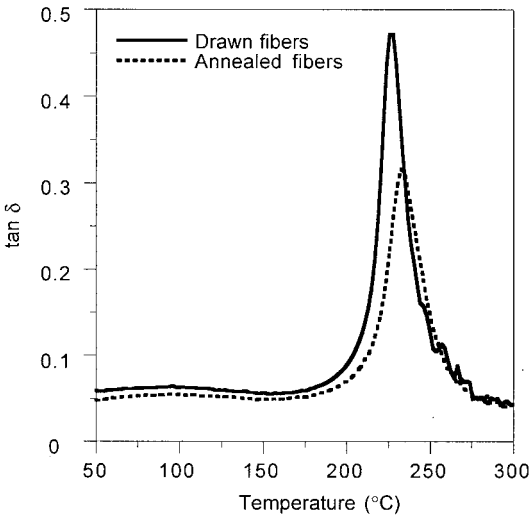

(a)

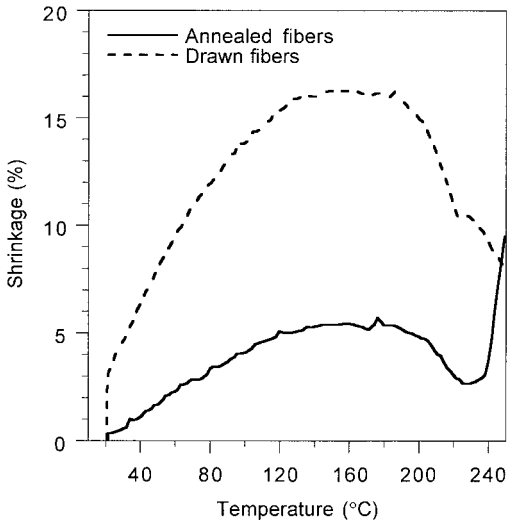

(b)

Figure 13 Dynamic mechanical spectroscopy and shrinkage of LaRC-IA drawn and annealed fibers (draw ratio = 5). (a) Loss tangent and (b) shrinkage.

1. The filaments, melt spun under conditions that produce low axial stress, are essentially amorphous. When heated even at a slow rate to temperatures well above the glass transition, no crystallization is observed in these fibers. This is consistent with the previously held notion that LaRC-IA is noncrystallizing, unless produced directly through precipitation/solidification from solution. However, the initially amorphous LaRC-IA filaments do crystallize rapidly if subjected to a sufficiently anisotropic stress field above their glass transition temperature. Anisotropic crystallization has been seen in thermal deformation analysis (force controlled) as well as in continuous drawing (deformation controlled).
2. Through anisotropic crystallization, the solid-like state of the polymer is extended well above its T_g to its melting point of 320°C, although the filaments still contain a significant fraction of noncrystalline phase.
3. As expected, the degree of anisotropy increases with deformation in continuous drawing. The relative effects of dominant relaxation of noncrystalline orientation and the constraints against it are seen, respectively, at low and high draw ratios. At higher draw ratios, the tensile strength increases fourfold to levels comparable to those of intermediate tenacity fibers of polyethylene terephthalate, polypropylene, nylon-6,6, and Nomex.
4. The significant anisotropy that evolves through drawing would also have its obvious consequences in producing anisotropy in dielectric properties, an aspect that might be beneficial in layered microelectronic structures.

REFERENCES

1. Li, F.; Wu, Z.-Q.; Savitski, E. P.; Jing, X.; Fu, Q.; Harris, F. W.; Cheng, S. Z. D.; Lyon, R. E. In Proceedings of the 42nd International SAMPE Symposium, Anaheim, CA, 1997; p 1306.
2. Irwin, R. S. U.S. Patent 3,415,782, E. I. duPont & Co., 1968.
3. Irwin, R. S. U.S. Patent 4,640,972, E. I. duPont & Co., 1987.
4. Kaneda, T.; Katsura, T.; Nakagawa, K.; Makino, H.; Horio, M. J Appl Polym Sci 1986, 32, 3133.
5. Dorogy, W. E., Jr.; St. Clair, A. K. J. Appl Polym Sci 1993, 49, 501.
6. Sroog, C. E. Progr Polym Sci 1991,16, 561.
7. M. Eashoo, D.-X. Shen, Z.-Q. Wu, F. W. Harris, S. Z. D. Cheng, K. H. Gardner and B. S. Hsiao, *Macromol. Chem.,* **195,** 2207 (1994).
8. D. Progar and T. L. St. Clair, J Adhesion Science and Technology, 1990, 4(7), 527.; US Patent 5 147 966, NASA Langley Research Center (Sept. 1992).
9. Fay, C. C.; Hinkley, J. A.; St. Clair, T. L.; Working, D. C. Advanced Performance Materials, to appear.
10. Working, D. C.; Marcello, T.; St. Clair, T. L. "Microextruder for Polymer Characterization"; NASA Langley Internal Paper, 1993.
11. Desai, P.; Abhiraman, A. S. J Polym Sci Part B Polym Phys Ed 1988, 26, 1657.
12. Dorsey, K. Master's Thesis, Georgia Institute of Technology, 1996.